Journal of Nuclear Materials 389 (2009) 68–71

Contents lists available at ScienceDirect

Journal of Nuclear Materials

journal homepage: www.elsevier.com/locate/jnucmat

Oxygen potential measurements of $Am_{0.5}Pu_{0.5}O_{2-x}$ by EMF method

Haruyoshi Otobe *, Mitsuo Akabori, Yasuo Arai

Nuclear Science and Engineering Directorate, Japan Atomic Energy Agency, Tokai-mura, Naka-gun, Ibaraki 319-1195, Japan

A B S T R A C T

The dependence of the oxygen potentials on oxygen non-stoichiometry and temperature of $Am_{0.5}Pu_{0.5}O_{2-x}$ has been obtained by the electromotive force (EMF) method with the cell: (Pt) air $|Zr(Ca)O_{2-x}|$ $Am_{0.5}Pu_{0.5}O_{2-x}$ (Pt). The x value of $Am_{0.5}Pu_{0.5}O_{2-x}$ was changed at 1333 K over $0.02 < x \leqslant 0.25$ by the coulomb titration method. The temperature dependence of the oxygen potential was also measured over the range of 1173–1333 K. It was found that the oxygen potential decreased from −80 to −360 kJ mol^{-1} with increasing x from 0.021 to 0.22 at 1333 K and that it remained almost constant at −360 $kJmol^{-1}$ around $x = 0.23$. It was concluded that $Am_{0.5}Pu_{0.5}O_{2-x}$ should be composed of the single fluorite-type phase over $0.02 < x \leqslant 0.22$ and the mixed phases of fluorite-type and $(Am,Pu)_9O_{16}$ at around $x = 0.23$.

1. Introduction

The transmutation of minor actinides (MA: Np, Am and Cm) by fast reactors can reduce the long-term hazard of the high-level radioactive waste. For the development of the oxide fuels containing MA, it is necessary to have an understanding of the oxygen potentials to predict the fuel-cladding compatibility and the thermodynamic behavior during irradiation. It is, therefore, important to determine the relation among the oxygen potentials, the crystal structure and the composition of MA-containing oxides.

In the previous study [1], we investigated the x and temperature dependences on the oxygen potentials of AmO_{2-x}. It was found that the oxygen potentials are sensitive to the phase relations.

For the next step, it is important to understand the relation among the oxygen potentials, the phase relations and the compositions of plutonium oxides containing Am, since ^{241}Am will always be present as a daughter of ^{241}Pu, $(U,Pu)O_{2-x}$ is considered as a potential driver fuel to burn MA and the understanding of the Am–Pu–O system is important to define the thermodynamic properties and phase equilibrium of the $(U,Pu,MA)O_{2-x}$ system.

The oxygen potentials of the fluorite-type plutonium oxide containing Am, with composition $Am_{0.09}Pu_{0.91}O_{2-x}$, have already been reported by Osaka et al. [2]. It was found that the oxygen potentials exhibited an anomalous change at around $x = 0.045$. Further, an effect of the interaction between Pu and Am on the oxygen potentials of $(Am,Pu)O_{2-x}$ was discussed. However, it is difficult to clarify the meaning of the anomalous change of the oxygen potentials in that study, because the Am content was so low and the x range investigated was narrow.

In the present study, therefore, we have investigated the oxygen potentials of $Am_{0.5}Pu_{0.5}O_{2-x}$, which is the equimolar solid solution of PuO_{2-x} and AmO_{2-x} over the wide x ranges of $0.02 < x \leqslant 0.25$ using the electromotive force (EMF) method, in order to clarify the relation among the oxygen potentials, the phase relations and the compositions of $(Am,Pu)O_{2-x}$. Systematic comparisons of the oxygen potentials between $Am_{0.5}Pu_{0.5}O_{2-x}$ and those published for AmO_{2-x} [1], $Am_{0.09}Pu_{0.91}O_{2-x}$ [2] and PuO_{2-x} [3] were also made.

2. Experimental

2.1. Sample preparation

$^{241}AmO_2$ powder was heated at 973 K in oxygen to remove the moisture from the powder, mixed with an equimolar amount of PuO_2 powder, ground in an agate mortar, and then pressed into pellets of 1 mm thickness and 3 mm diameter at a pressure of 400 MPa. The mass of one pellet was about 100 mg. The pellets were sintered for 48 h at 1650 K in flowing dry air, followed by heating for 1 h at 1333 K in flowing dry air to control the oxygen-stoichiometry (x) of the sample.

One of the prepared pellets was crushed into powder and analyzed by the powder X-ray diffraction (XRD) method at room temperature with Mo-kα radiation (diffractometer: Rigaku Denki Co. Ltd., Japan) within 24 h after heating at 1333 K in order to avoid the lattice damage due to the decay of Am and Pu.

2.2. Oxygen potential measurements using the EMF method

The oxygen potential measurement system used in the present study is the same as that used in the previous study for AmO_{2-x} [1]. The system has been described in detail in a previous publication literature [1]. The oxygen potentials were measured by the EMF

---

* Corresponding author. Tel.: +81 29 282 5488; fax: +81 29 282 5935.
E-mail address: otobe.haruyoshi@jaea.go.jp (H. Otobe).

0022-3115/$ - see front matter © 2009 Elsevier B.V. All rights reserved.
doi:10.1016/j.jnucmat.2009.01.009

method using a zirconia solid-electrolyte (type: ZR-11, Nikkato Co., Japan).

The arrangement of the galvanic cell used in the present study was

$$(\text{Pt-electrode})Am_{0.5}Pu_{0.5}O_{2-x}/Zr(Ca)O_{2-x}/\text{air}(\text{Pt-electrode}).$$

The oxygen potentials of the sample, $\Delta\overline{G}_{O_2}$ are given in the following equation:

$$\Delta\overline{G}_{O_2} = RT\ln P_{O_2},$$

where R is the gas constant, T is the temperature, P_{O_2} is the equilibrium partial pressure of oxygen for the sample.

In this equation the Nernst equation is put: the Nernst equation is

$$E = -(RT/|Z|F)\cdot \ln(P_{O_2}/P_{O_2}^{\text{air}}),$$

where E is the potential difference between two Pt-electrodes, $|Z|$ is the charge number corresponding to an oxygen molecule (=4), F is the Faraday constant, and $P_{O_2}^{\text{air}}$ is the partial pressure of oxygen in air (0.206 atm).

Then, the oxygen potential is also written as

$$\Delta\overline{G}_{O_2} = |Z|FE + RT\cdot \ln P_{O_2}^{\text{air}}.$$

The E values were measured with a potentio/galvanostat (precision: 0.02 mV, SI1280, Solartron, UK) and an electrometer (precision: 0.002 mV, 6514, Keithley Instruments Inc., US). The temperature of the sample was measured by using a digital thermometer (precision: 0.1 K, 2575, Yokogawa Electric Corporation, Japan) with a thermocouple (type: Pt-PtRh13%, precision: 0.007 mV, Tanaka Kikinzoku Kogyo K.K., Japan).

The E value was measured for 6 h after the coulometric titration, in order to monitor the effect of oxidation (or reduction) on the E value by a small amount of contaminant in the purified helium gas during the coulometric titration. The E value was corrected by eliminating this effect [4].

The oxygen potentials of CeO_{2-x} obtained in the preparatory study agreed with the literature data [5] with a maximum error of 2 kJ mol^{-1} for the corresponding x value and temperature. Therefore, the maximum error of the oxygen potentials of $Am_{0.5}Pu_{0.5}O_{2-x}$ in the present study was considered to be within 2 kJ mol^{-1}.

2.3. Temperature dependence

The temperature stepwise scan was also conducted: cooling from 1333 K to the target temperature, which was set from 1293 to 1173 K at the interval of 40 K, at the rate of 4 K min^{-1} and holding the target temperature for 1 h, then heating again to 1333 K at the same rate as the cooling. The oxygen potentials during the heating and cooling at each temperature were averaged in order to eliminate the effect of the contaminant from the measured oxygen potentials.

3. Results and discussion

3.1. XRD analysis

The prepared sample treated by heating in dry air at 1333 K was identified as the single fluorite-type phase (Space group: Fm $\overline{3}$ m) by the XRD pattern. The lattice parameter was evaluated to be 0.5383 ± 0.0001 nm by means of the least-squares method. The XRD pattern suggests that $Am_{0.5}Pu_{0.5}O_{2-x}$ with the oxygen potential equal to −17.511 kJ mol^{-1} at 1333 K should have the single fluorite-type structure, if the structure or the oxygen stoichiometric composition did not change during the cooling from 1333 K to room temperature.

3.2. Isothermal curve of the oxygen potential

Fig. 1 shows the oxygen potentials of $Am_{0.5}Pu_{0.5}O_{2-x}$ at 1333 K as a function of x obtained by the coulometric titration method. The oxygen potentials of AmO_{2-x} [1] and PuO_{2-x} [3] in literature are also shown for comparison in Fig. 1. The oxygen potentials of $Am_{0.5}Pu_{0.5}O_{2-x}$ at 1333 K smoothly decreased from −80 to −360 kJ mol^{-1} with increasing x from 0.02 to 0.22, remained almost constant at −360 kJ mol^{-1} around $x = 0.23$ and decreased again from −360 to −420 kJ mol^{-1} with increasing x from 0.23 to 0.25. In this context, the isothermal curve of the oxygen potentials of $Am_{0.5}Pu_{0.5}O_{2-x}$ over the x range of $0.02 < x \leqslant 0.25$ at 1333 K exhibited the similarity to those of AmO_{2-x} [1] over the corresponding x and temperature ranges. Therefore, the phase relations of $Am_{0.5}Pu_{0.5}O_{2-x}$ over this x range at 1333 K are supposed to be similar to those of AmO_{2-x} [1]. The phase relations of $Am_{0.5}Pu_{0.5}O_{2-x}$ were speculated from the oxygen potentials of $Am_{0.5}Pu_{0.5}O_{2-x}$ and the phase relations of AmO_{2-x} [1]. In the phase relations of $Am_{0.5}Pu_{0.5}O_{2-x}$ at 1333 K, the single fluorite-type phase should be dominant over the x range of $0.02 < x \leqslant 0.22$ at 1333 K, $Am_{0.5}Pu_{0.5}O_{2-x}$ should be decomposed into the mixed phases of the fluorite-type $(Am,Pu)O_{2-x}$, and the intermediate stable $(Am,Pu)_9O_{16}$ around $x = 0.23$, and the single fluorite-type phase should be dominant again over the x range of $0.23 < x \leqslant 0.25$.

Some oxygen potential plots are diverged from the flat line at −360 kJ mol^{-1} and around $x = 0.23$. This indicates that the oxygen potential data contained not only those of the equilibrium phase but also those of the non-equilibrium phase, because the coulometric titration method can insert and extract oxide ions into and out of an oxide lattice even if it is in a non-equilibrium state [6].

The oxygen potential plots over the x range of $0.23 < x \leqslant 0.25$ are somewhat scattered, which has not been seen in our previous study of AmO_{2-x} [1]. This means these data of $Am_{0.5}Pu_{0.5}O_{2-x}$ also contained the oxygen potentials of a non-equilibrium phase in addition to those of the equilibrium phase. The temperature of 1333 K may be too low for the cations to smoothly rearrange to the most stable configuration within 6 h after the coulometric titration. Pu^{4+} ions with the relatively small ionic radius [7] cannot be easily replaced by Am^{3+} ions with the relatively large ionic radius [7] at 1333 K, even if the replacement leads to the stability of the crystal structure of $Am_{0.5}Pu_{0.5}O_{2-x}$, while Am^{4+} ions can be

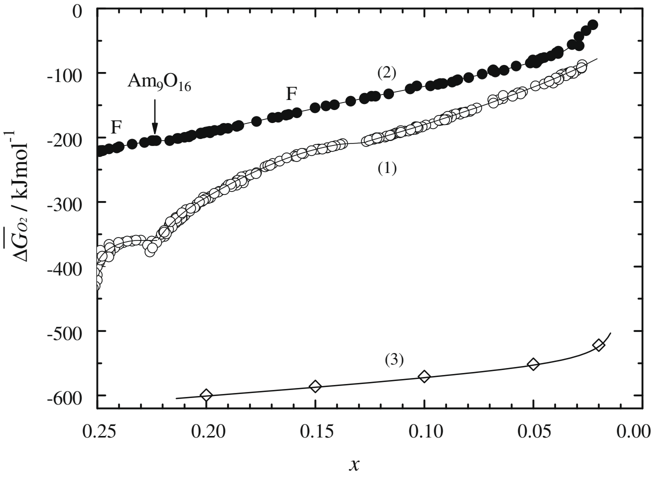

Fig. 1. The oxygen potentials of $Am_{0.5}Pu_{0.5}O_{2-x}$, AmO_{2-x} and PuO_{2-x} at 1333 K as a function of x. (1) $Am_{0.5}Pu_{0.5}O_{2-x}$ in the present study, (2) AmO_{2-x} [1], (3) PuO_{2-x} [3]. F: the fluorite-type phase region in Am–O system [1]. Am_9O_{16}: the Am_9O_{16} phase in Am–O system [1].

easily replaced by Am^{3+} ions only through the exchange of electrons in the crystal structure of AmO_{2-x}.

The oxygen potentials of $Am_{0.5}Pu_{0.5}O_{2-x}$ were lower than those of AmO_{2-x} by approximately 60 kJ mol^{-1} at the corresponding x at 1333 K over the x range of $0.02 < x \leqslant 0.22$, whereas they were higher than those of PuO_{2-x} by approximately 300 kJ mol^{-1}.

As shown in Fig. 1, the oxygen potentials of $Am_{0.5}Pu_{0.5}O_{2-x}$ steeply dropped around -420 kJ mol^{-1} with increasing x. The x value corresponding to the oxygen potential of -420 kJ mol^{-1} was taken to be 0.25 and used as a reference to determine all the x values of the isothermal curve of the oxygen potentials for $Am_{0.5}Pu_{0.5}O_{2-x}$. It is assumed that for $x = 0.25$, i.e., at the composition of $Am_{0.5}Pu_{0.5}O_{1.75}$, all Am ions took +3 valence, that the oxygen potentials no longer depended on the oxidation-reduction of Am^{+3} and Am^{4+} ions, and that the oxidation-reduction of Pu^{4+} and Pu^{3+} ions had not yet occurred, considering that the oxygen potentials of PuO_{2-x} [3] are lower than -420 kJ mol^{-1}. This should be the reason for the steep drop around the oxygen potential of -420 kJ mol^{-1}.

The oxygen potentials of $Am_yPu_{1-y}O_{2-x}$ at 1333 K as a function of x/y for $y = 0.5$ ($Am_{0.5}Pu_{0.5}O_{2-x}$) and $y = 1$ (AmO_{2-x}) [1] are shown in Fig. 2. The oxygen potentials of $Am_{0.5}Pu_{0.5}O_{2-x}$ and AmO_{2-x} agree fairly well with each other at the corresponding x/y over the x/y range of $0.04 \leqslant x/y \leqslant 0.27$. This result reveals that the oxygen potentials of $(Am,Pu)O_{2-x}$ over this x/y range should not depend on the oxidation-reduction of Pu ions ($Pu^{4+} \leftrightarrow Pu^{3+}$) but on that of Am ions ($Am^{4+} \leftrightarrow Am^{3+}$), when they have the single fluorite-type structures.

The AmO_{2-x} phase is different from the single fluorite-type for $x/y > 0.27$, whereas the $Am_{0.5}Pu_{0.5}O_{2-x}$ phase remains the single fluorite-type over this x/y range. Therefore, the difference of the oxygen potentials between them should become significant for $x/y > 0.27$.

The oxygen potentials of $Am_{0.09}Pu_{0.91}O_{2-x}$ at 1273 and 1423 K [2] are also shown in Fig. 2. Those of $Am_{0.09}Pu_{0.91}O_{2-x}$ [2] and $Am_{0.5}Pu_{0.5}O_{2-x}$ obtained in the present study agree well with each other especially when the oxygen potentials is higher than -150 kJ mol^{-1} for $x/y < 0.1$ and lower than -300 kJ mol^{-1} for $x/y > 0.4$. Both of $Am_{0.5}Pu_{0.5}O_{2-x}$ and $Am_{0.09}Pu_{0.91}O_{2-x}$ have the single fluorite-type structures almost all over these x/y ranges.

For $0.1 < x/y < 0.4$ there is apparently the discrepancy of the oxygen potentials between $Am_{0.09}Pu_{0.91}O_{2-x}$ and $Am_{0.5}Pu_{0.5}O_{2-x}$ at the corresponding x/y. However, the oxygen potentials of $Am_{0.09}Pu_{0.91}O_{2-x}$ were measured in the thermogravimetric analysis, which needs the strict control of gas compositions corresponding to the oxygen partial pressure [2]. It might be difficult to control the oxygen partial pressure corresponding to the oxygen potentials from -150 to -300 kJmol^{-1} by using H_2O/H_2 gas equilibrium and dilute O_2 gas in the manner of Osaka et al. [2], because the H_2O/H_2 gas equilibrium is subject to the highest limit of water vapor pressure and the dilute O_2 gas is subject to the lowest limit of the O_2 content to control, the interference of the active contaminants in the gas and the long time for the sample to equilibrate to the dilute O_2 gas. In order to control the oxygen partial pressure corresponding to the oxygen potentials from -150 to -300 kJ mol^{-1}, the CO/CO_2 or H_2/CO_2 gas equilibria should be used. If these mixed gas equilibria were used, the difficulty described above should not have occurred.

The difficulty might cause the small discrepancy of the oxygen potentials between $Am_{0.5}Pu_{0.5}O_{2-x}$ and $Am_{0.09}Pu_{0.91}O_{2-x}$ [2] over the range of the oxygen potential from -150 to -300 kJ mol^{-1}, i.e., for $0.1 \leqslant x/y \leqslant 0.4$. The oxygen potentials of $Am_{0.09}Pu_{0.91}O_{2-x}$ have the possibility to be similar to those of $Am_{0.5}Pu_{0.5}O_{2-x}$ for $0.1 \leqslant x/y \leqslant 0.4$, besides for $x/y < 0.1$ and $x/y > 0.4$.

Therefore, the oxygen potentials of $Am_{0.09}Pu_{0.91}O_{2-x}$ [2] are consistent with the conclusion that the oxygen potentials of $(Am,Pu)O_{2-x}$ should not depend on the oxidation-reduction of Pu ions ($Pu^{4+} \leftrightarrow Pu^{3+}$) but depend on that of Am ions ($Am^{4+} \leftrightarrow Am^{3+}$), which was revealed by the comparison between $Am_{0.5}Pu_{0.5}O_{2-x}$ and AmO_{2-x}.

3.3. Temperature dependence of the oxygen potential

Fig. 3 shows the temperature dependence of the oxygen potential of $Am_{0.5}Pu_{0.5}O_{2-x}$ for $x = 0.029$, 0.087, 0.148, 0.187, 0.207, near 0.23 and 0.248. The x values were deduced from the isothermal curve of the oxygen potential at 1333 K shown in Fig. 1.

For $x = 0.029$, the oxygen potentials smoothly decreased with decreasing temperature. This result suggests that $Am_{0.5}Pu_{0.5}O_{2-x}$ should keep the single fluorite-type phase from 1333 to 1173 K.

For $x = 0.087$, 0.148 and 0.187, the oxygen potential decreased with decreasing temperature from 1333 to 1250 K and afterward increased with decreasing temperature from 1250 to 1173 K. The phase should change from the single fluorite-type $Am_{0.5}Pu_{0.5}O_{2-x}$ to the two fluorite-type phases of $(Am,Pu)O_{2-x'}$ and $(Am,Pu)O_{2-x''}$ around 1250 K, considering the phase relations of AmO_{2-x}.

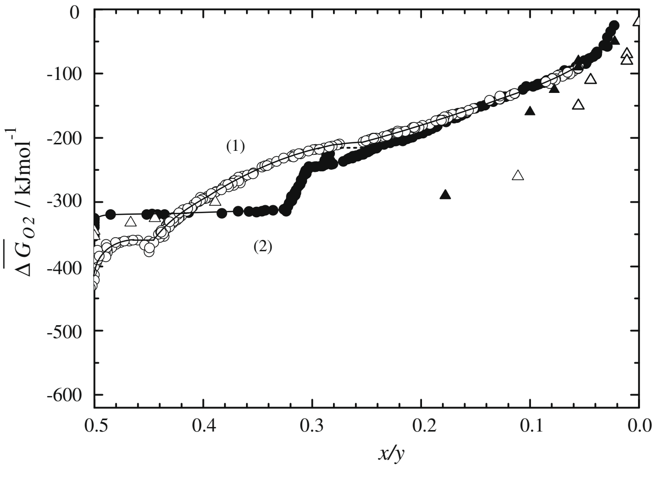

Fig. 2. The oxygen potentials of $Am_yPu_{1-y}O_{2-x}$ as a function of x/y. (1) $Am_{0.5}Pu_{0.5}O_{2-x}$ at 1333 K in the present study, (2) AmO_{2-x} at 1333 K [1], (△) $Am_{0.09}Pu_{0.91}O_{2-x}$ at 1273 K [2], (▲) $Am_{0.09}Pu_{0.91}O_{2-x}$ at 1423 K [2].

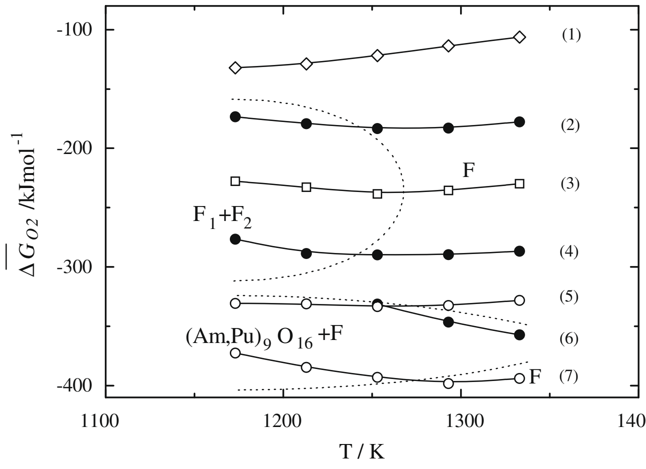

Fig. 3. The temperature dependence of the oxygen potentials of $Am_{0.5}Pu_{0.5}O_{2-x}$ and the phase. (1) $x = 0.029$, (2) $x = 0.087$, (3) $x = 0.148$, (4) $x = 0.187$, (5) $x = 0.207$, (6) x = near 0.23, (7) $x = 0.248$. (—): the equilibrium line deduced from the experimental data in the present study. (————): the tentative phase boundary deduced from the experimental data in the present study. F, F_1 and F_2: the fluorite-type phase region. $(Am,Pu)_9O_{16}$: the $(Am,Pu)_9O_{16}$ phase region.

For $x = 0.207$, the oxygen potential decreased with decreasing temperature from 1333 to 1250 K and kept constant with decreasing temperature from 1250 to 1173 K. The phase should change form the single fluorite-type $Am_{0.5}Pu_{0.5}O_{2-x}$ to the fluorite-type $(Am,Pu)O_{2-x'}$ and $(Am,Pu)_9O_{16}$ around 1250 K.

Around $x = 0.23$, the oxygen potential increased with decreasing temperature from 1333 to 1253 K. This suggested that the phase should be in non-equilibrium at 1333 K; the non-equilibrium phase may be the single fluorite-type $(Am,Pu)O_{2-x}$, whereas the equilibrium phase is composed of the fluorite-type $(Am,Pu)O_{2-x'}$ and $(Am,Pu)\ _9O_{12}$ as described above.

For $x = 0.248$, the oxygen potential decreased with decreasing temperature from 1333 to 1280 K and increased with decreasing temperature from 1280 to 1173 K. The phase should change from the single fluorite-type $Am_{0.5}Pu_{0.5}O_{2-x}$ to the fluorite-type $(Am,Pu)O_{2-x'}$ and $(Am,Pu)_9O_{16}$ around 1280 K.

The temperature dependence of the oxygen potential of $Am_{0.5}Pu_{0.5}O_{2-x}$ was consistent with the isothermal curve of the oxygen potentials at 1333 K shown in Fig. 1 and can be explained consistently by the substitution of the phase diagram of Am–O system. The phase relations derived from the results of the oxygen potential measurements in the present study were also shown in Fig. 3, although they were tentative.

4. Conclusion

In the present study, the oxygen potentials of $Am_{0.5}Pu_{0.5}O_{2-x}$ were investigated by an EMF method with a zirconia oxygen sensor over the x range of $0.02 < x \leqslant 0.25$ between 1173 and 1333 K. It was found that the oxygen potentials smoothly decreased with increasing x from 0.02 to 0.22, remained almost constant around $x = 0.23$ and again decreased with increasing x from 0.23 to 0.25. In this context, the isothermal curve of the oxygen potentials of $Am_{0.5}Pu_{0.5}O_{2-x}$ over the range of x from 0.02 to 0.25 at 1333 K exhibited the similarity to those of AmO_{2-x} over the corresponding x and temperature ranges. Therefore, the phase relations of $Am_{0.5}Pu_{0.5}O_{2-x}$ should be similar to those of AmO_{2-x} at 1333 K over $0.02 < x \leqslant 0.25$.

The temperature dependence of the oxygen potential of $Am_{0.5}Pu_{0.5}O_{2-x}$ between 1173 and 1333 K over the x range of $0.02 < x < 0.25$ can be also explained by the substitution of the phase diagram of Am–O system, although the experimental data contained some of the non-equilibrium phases.

Acknowledgements

The present study is part of the programme "The development of common and fundamental technologies on the evaluation of nuclear fuel behavior for realizing MA recycling" implemented by the Japan Atomic Energy Agency for the Ministry of Education, Culture, Sports, Science and Technology of Japan (MEXT).

References

[1] H. Otobe, M. Akabori, K. Minato, J. Am. Ceram. Soc. 91 (6) (2008) 1981.
[2] M. Osaka, K. Kurosaki, S. Yamanaka, J. Nucl. Mater. 357 (2006) 69.
[3] R.E. Woodley, J. Nucl. Mater. 96 (1981) 5.
[4] H. Otobe, A. Nakamura, T. Yamashita, T. Ogawa, J. Nucl. Sci. Technol. (Suppl. 3) (2002) 652.
[5] D.J.M. Bevan, J. Kordis, J. Inorg. Nucl. Chem. 26 (1964) 1509.
[6] J.B. Thomson, A.R. Armstrong, P.G. Bruce, J. Am. Chem. Soc. 118 (1996) 11129.
[7] R.D. Shannon, Acta Crystallogr., Sect. A A32 (5) (1976) 751.